Fatigue Crack Paths in Ferritic-Perlitic Ductile Cast Irons

F. Iacoviello and V. Di Cocco

Università di Cassino, Di.M.S.A.T., via G. Di Biasio 43, 03043 Cassino (FR) ITALY, iacoviello@unicas.it

ABSTRACT. *Ductile iron discovery in 1948 gave a new lease on life to the cast iron family. In fact these cast irons are characterised both by a high castability and by high toughness values, combining cast irons and steel good properties. Ductile cast irons are also characterised by high fatigue crack propagation resistance, although this property is still not widely investigated. In the present work we considered three different ferritic-perlitic ductile cast irons, characterised by different ferrite/perlite volume fractions. Their fatigue crack propagation resistance was investigated by means of fatigue crack propagation tests according to ASTM E647 standard, considering three different stress ratios ($R = K_{min}/K_{max} = 0.1; 0.5; 0.75$). Crack surfaces were extensively analysed by means of a scanning electron microscope. Crack paths were investigated by means of a crack path profile analysis performed by means of an optical microscope. In order to analyse ferrite/perlite volume fractions and graphite spheroids influence, da/dN-ΔK fatigue crack propagation results were compared with profile and fracture surface analysis.*

INTRODUCTION

In the first half of the last century, the goals of a combination of good castability and high toughness values were fulfilled by malleable iron by means of an extended annealing treatment of white iron. During this heat treatment, cementite decomposes to graphite that precipitates as aggregates in a matrix whose composition (ferrite or pearlite) depending on the cooling cycle from the annealing temperature. The high costs related to the extended annealing treatment required and the difficulty to cast sound white iron components limited its utilization. In 1943, in the International Nickel Company Research Laboratory, a magnesium addition allowed to obtain a cast iron containing not flakes but nearly perfect graphite spheres. In 1948, a small amount of cerium allowed to obtain the same result. These cast irons are characterised by a very good combination of overall properties: high ductility (up to more than 18%), high strength (up to 850 MPa and, considering austempered ductile iron, up to 1600 MPa) and good wear resistance. Matrix controls these good mechanical properties and matrix names are used to designate spheroidal cast iron types. Ferritic ductile irons are characterised by good ductility and a tensile strength that is equivalent to a low carbon steel. Perlitic ductile irons shows high strength, good wear resistance and moderate ductility. Ferritic-perlitic grades properties are intermediate between ferritic and perlitic

ones. Martensitic ductile irons show very high strength, but low levels of toughness and ductility. Bainitic grades are characterised by a high hardness. Austenitic ductile irons show good corrosion resistance, good strength and dimensional stability at high temperature. Austempered grades show a very high wear resistance and fatigue strength [1, 2].

Ductile cast irons are widely used in a number of industries, e.g. wheels, gears, crankshafts in cars and trucks etc.

In this work the fatigue crack path in three different ferritic-perlitic ductile irons were investigated, in order to characterise the fatigue crack propagation micromechanism.

MATERIALS AND EXPERIMENTAL METHODS

Three different ferritic-perlitic ductile irons were considered with the chemical compositions of Tables 1 to 3.

Table 1. Ductile iron GS350-22 chemical composition (100% ferrite).

C	Si	Mn	S	P	Cu	Cr	Mg	Sn
3,66	2,72	0,18	0,013	0,021	0,022	0,028	0,043	0,010

Table 2. Ductile iron GS500-7 chemical composition (50% ferrite – 50% perlite).

C	Si	Mn	S	P	Cu	Cr	Mg	Sn
3,65	2,72	0,18	0,010	0,03	-	0,05	0,055	0,035

Table 3. Ductile iron GS700-2 chemical composition (5% ferrite – 95% perlite).

C	Si	Mn	S	P	Cu	Mo	Ni	Cr	Mg	Sn
3,59	2,65	0,19	0,012	0,028	0,04	0,004	0,029	0,061	0,060	0,098

Fatigue tests were run according to ASTM E647 standard [3], using CT (Compact Type) 10 mm thick specimens and considering three different stress ratio values (e.g. R = P_{min}/P_{max} = 0.1; 0.5; 0.75). Tests were performed using a computer controlled INSTRON 8501 servohydraulic machine in constant load amplitude conditions, using a 20 Hz loading frequency, a sinusoidal waveform and laboratory conditions. Crack length measurements were performed by means of a compliance method using a double cantilever mouth gage and controlled using an optical microscope (x40). Fracture surfaces were analysed by means of a Philips scanning electron microscope (SEM). Fatigue crack path analyses were conducted using specimens tested at R = 0.5, by means of an optical microscope (x200), according to the following procedure:

- Fracture surface nickel coating (in order to protect fracture surface during cutting);
- Fractured specimen longitudinal cutting, at half thickness, along the fatigue crack propagation direction (by means of a diamond saw);

- Metallographic preparation of the section (up to 0.2 μm Al_2O_3 powder solution)
- Nital 4 etching (5 seconds).

RESULTS AND DISCUSSION

Stress ratio influence on ferritic-perlitic ductile irons fatigue crack propagation is shown in Figs 1 to 3. For all the investigated ductile cast irons, considering the fatigue crack growth at constant ΔK values, fatigue crack growth rate da/dN increases with the stress ratio. This behaviour is due to crack closure effect that can be crack tip plasticity, oxide forming and/or fracture surface roughness induced [4, 5]. Roughness surface analysis and scanning electron microscope (SEM) fracture surface investigation [6, 7] show a low influence of the oxide forming and fracture surface roughness induced crack closure effect. Considering lower R values (e.g. R = 0.1) or lower ΔK values (near threshold), fatigue crack propagation is not influenced by matrix microstructure. Higher R or ΔK values imply an increase of the matrix microstructure influence on fatigue crack propagation resistance, with the 50% ferrite – 50% perlite ductile iron showing the best behaviour. Fatigue crack surface SEM analysis and fatigue crack path investigation show different fatigue crack propagation micromechanisms depending on the ductile iron microstructure (Figs 4 to 11; crack propagates from left to right).

Fatigue crack propagation micromechanisms in ferritic ductile iron are connected both to the ductile striation generation and to an evident cleavage (Fig. 4), for all the loading condition (not depending on R or ΔK). Furthermore, a graphite spheroids debonding is shown both for lower and for higher ΔK and R values (Fig. 5).

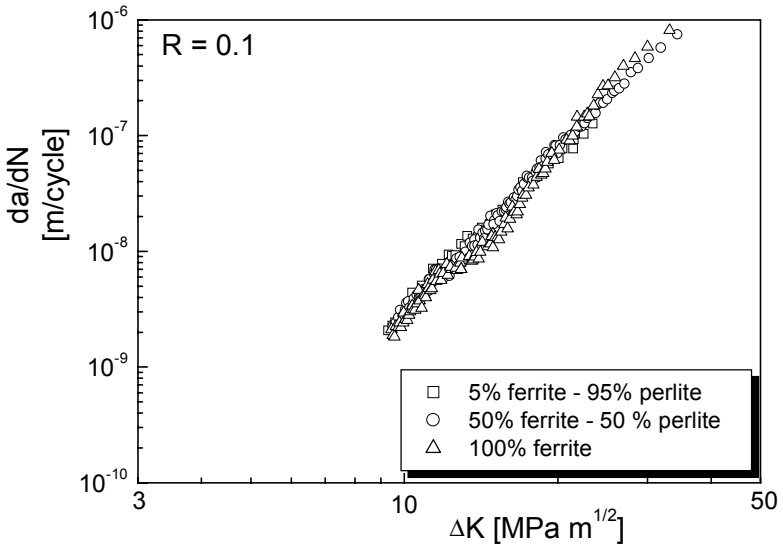

Figure 1. Fatigue crack propagation results for the investigated ductile irons (R = 0.1).

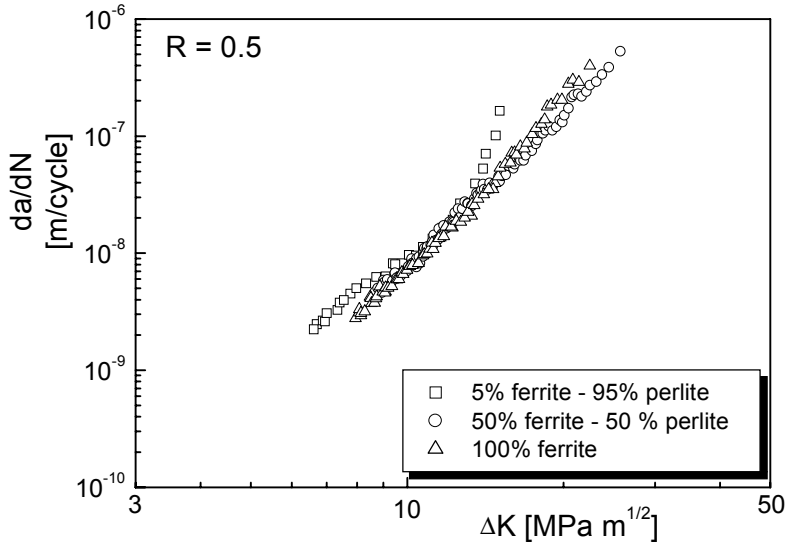

Figure 2. Fatigue crack propagation results for the investigated ductile irons (R = 0.5).

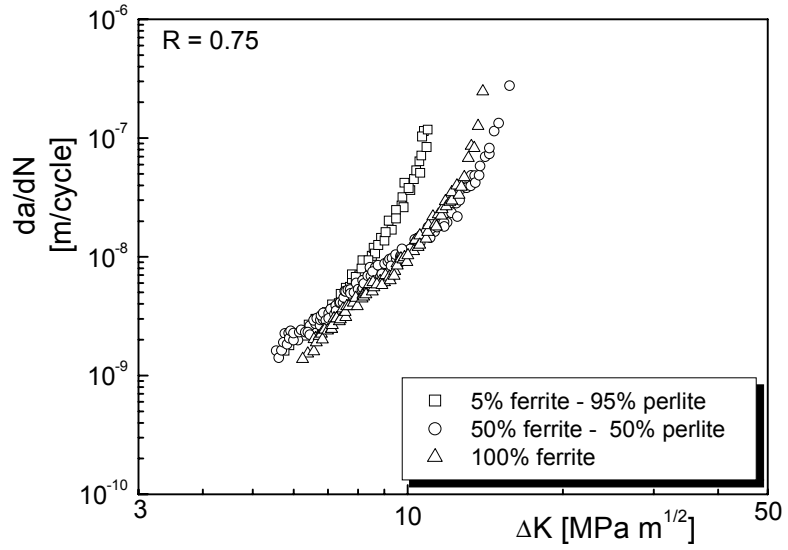

Figure 3. Fatigue crack propagation results for the investigated ductile irons (R = 0.75).

This debonding does not imply automatically a complete spheroid loosing from the surface. Also spheroids that have less that half of their surface in contact with ferritic matrix do not loose their grip to the surface.

As a consequence, the closure effect is enhanced by the graphite spheroids presence. If the spheroid looses completely the grip with the ferritic matrix, the matrix ductile deformation implies an increase of the hole dimension with a mechanism that is similar

to the microvoid growing in dimples formation. If the debonding is not complete, also the void growing is not complete, but however evident (Fig. 5).

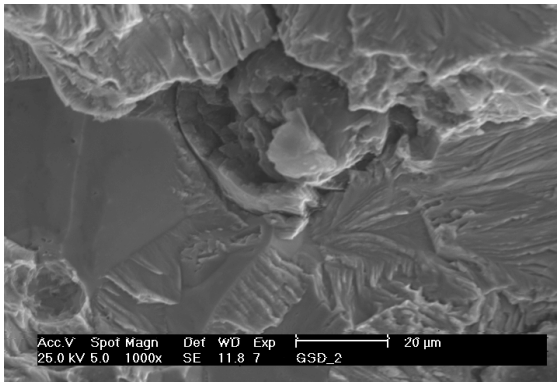

Figure 4. SEM fractography (100% ferrite; R = 0.5; ΔK = 10 MPa √m).

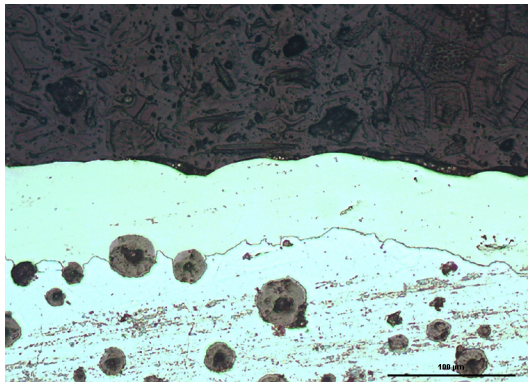

Figure 5. Optical microscope fracture surface profile analysis (100% ferrite; R = 0.5; ΔK = 10 MPa √m).

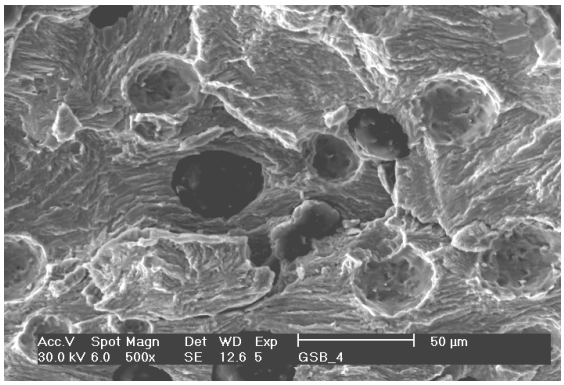

Figure 6. SEM fractography (5% ferrite, 95% perlite; R = 0.5; ΔK = 10 MPa √m).

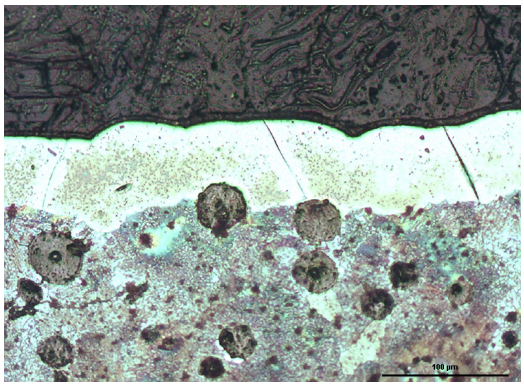

Figure 7. Optical microscope fracture surface profile analysis (5% ferrite, 95% perlite; R = 0.5; ΔK = 10 MPa √m).

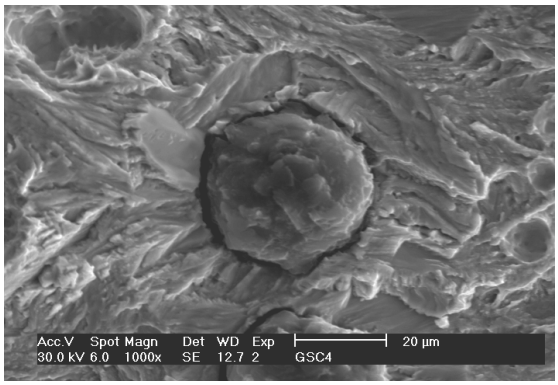

Figure 8. SEM fractography (50% ferrite, 50% perlite; R = 0.5; ΔK = 10 MPa √m).

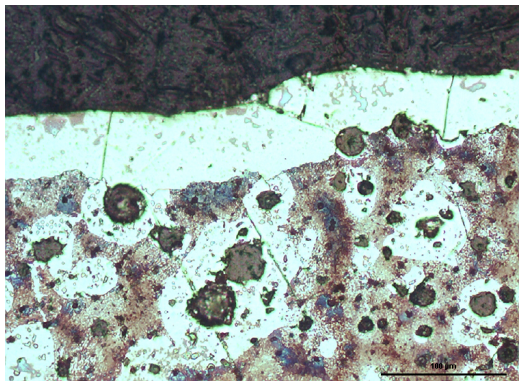

Figure 9. Optical microscope fracture surface profile analysis (50% ferrite, 50% perlite; R = 0.5; ΔK = 10 MPa √m).

Perlitic ductile iron shows a different fracture surface morphology, that always does not depend on ΔK or R values. Secondary cracks and ductile and fragile striations are the main fatigue crack propagation micromechanisms (Fig. 6). Graphite spheroids debonding is often complete, and no void growing is observed (Fig. 7). Spheroid gripping on fracture surface is possible only if at least half of the spheroid surface is in contact with the perlitic matrix, but this condition is not sufficient. After this spheroid "fragile" debonding, it is possible to observe that the surface inside the hole shows an evident microductility, consisting in a microdimples generation.

Ferritic-perlitic ductile iron shows fatigue crack propagation micromechanisms that are influenced by its microstructure. Ferritic shields are often fractured by cleavage and perlitic matrix shows the same fracture morphology of the fully perlitic ductile iron. No evidence of secondary cracks is observed (Fig. 8). Graphite spheroids debonding depends on the loading conditions and is evidently influenced by the metal matrix. Considering lower ΔK values, fracture profile does not show a void growing (Fig. 9) as in perlitic ductile iron. Considering higher applied ΔK values, the ferritic shield is more an more stressed and the ductile debonding becomes more and more evident (Figs 10 and 11). As a consequence of this ductile debonding, graphite spheroids act as crack closure effect raisers, as in ferritic ductile iron. The influence of metal matrix microstructure on graphite spheroids debonding is summarised in Fig. 12.

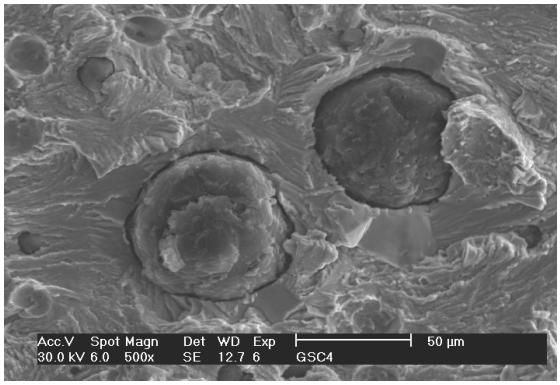

Figure 10. SEM fractography (50% ferrite, 50% perlite; R = 0.5; ΔK = 20 MPa √m).

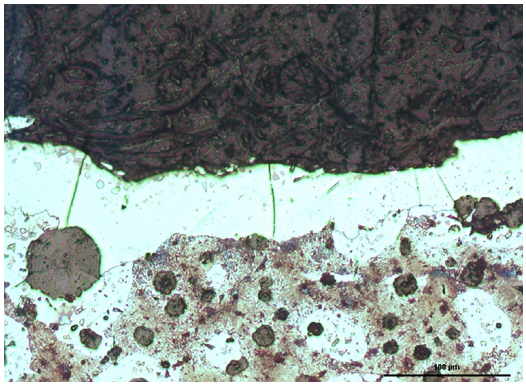

Figure 11. Optical microscope fracture surface profile analysis (50% ferrite, 50% perlite; R = 0.5; ΔK = 10 MPa √m).

Considering ferritic-perlitic ductile iron, a second peculiar closure effect is due to the different mechanical behaviour of the ferritic shields (more ductile) and of the perlitic matrix (more fragile). In fact during the loading cycle, the ferrite and perlite deformation level could be really different, especially for higher R and ΔK values:

- corresponding to K_{max} values, ferritic shields are more deformed than perlitic matrix;
- corresponding to K_{min} values, perlitic matrix induces on ferritic shields a residual compression stress condition with a consequent enhancing of the closure effect (Fig. 12).

Considering both the fatigue crack propagation tests results (Figs 1 to 3) and the fatigue crack propagation micromechanisms investigation and the evidence of the influence of different crack closure mechanisms depending on the matrix microstructure and on the spheroids presence, it is possible to outline that the higher fatigue crack propagation resistance of the ferritic-perlitic ductile iron depends on the crack closure mechanisms. Higher R and ΔK values enhance the matrix microstructure and spheroids influence. For these loading conditions:

- graphite spheroids ductile debonding in ferritic and ferritic-perlitic ductile iron implies a "spheroid presence induced" crack closure effect.
- the different mechanical behaviour of ferrite and perlite, and the peculiar distribution of these two phases in ferritic-perlitic ductile iron, implies an increasing of the importance of the crack tip plasticity induced crack closure effect that acts on ferritic shields.

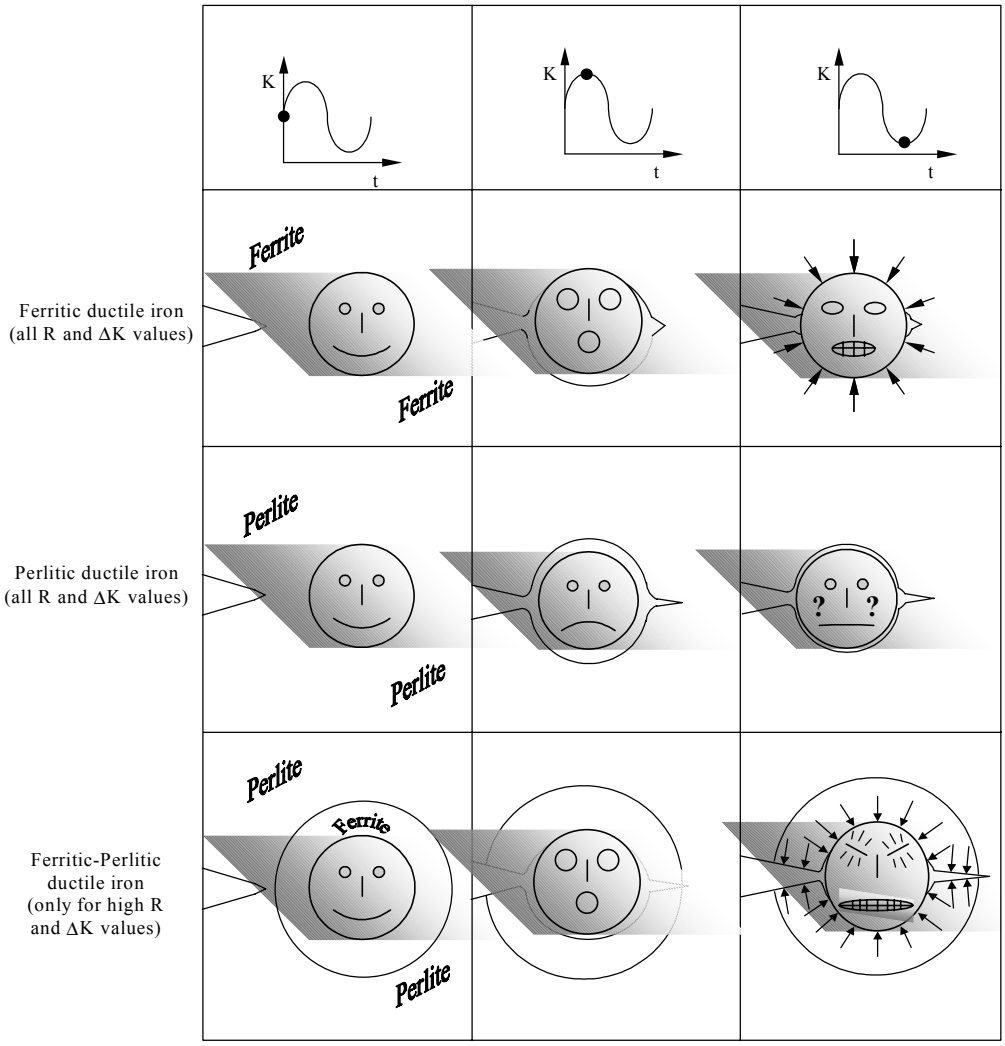

Figure 12. Ductile and fragile debonding models for the three investigated ductile irons: influence of a graphite spheroid.

CONCLUSIONS

The aim of this work was the analysis of the microstructure influence on ferritic-perlitic ductile iron fatigue crack propagation. This analysis was performed by means of fatigue crack propagation tests according to ASTM E647 standard, considering three different ductile irons (from fully ferritic to almost fully perlitic), and three different stress ratio (R = 0.1; 0.5; 0.75). A complete SEM fracture surface investigation and the analysis of fatigue crack path were performed. On the basis of the experimental analysis, the following conclusions can be summarised:

- Fatigue crack propagation micromechanisms depend on the spheroids presence, ferrite/perlite volume fractions and loading conditions; the higher the ΔK and R values, the strongest the microstructure influence is.
- Considering the ferritic and the ferritic-perlitic ductile irons, the presence of graphite spheroids could imply a "graphite spheroids presence" induced crack closure effect. This is due to a ductile graphite spheroids debonding. Fully perlitic ductile iron is characterised by a "fragile" spheroid debonding.
- Ferritic-perlitic ductile iron shows a second peculiar closure effect that is due to the different mechanical behaviour of the ferritic shields (more ductile) and of the perlitic matrix (more fragile). As a consequence, a residual compression stress condition in ferritic shields could imply a decreasing of fatigue crack growth.

ACKNOWLEDGEMENTS

Fonderghisa S.p.A. is acknowledged.

REFERENCES

1. Ward, R.G. (1962) *An introduction to the physical chemistry of iron and steel making,* Arnold, London.
2. Labrecque, C. and Gagne, M. (1998) *Canadian Metallurgical Quarterly*, 37, 5, 343-378.
3. *ASTM Standard test Method for Measurements of fatigue crack growth rates (E647-93)*, Annual Book of ASTM Standards, (1993), 0301, American Society for Testing and Materials.
4. Elber, W. (1971) *ASTM STP 486*, 280-289.
5. Ritchie, R.O. and Suresh, S. (1982) *Metall. Trans. A* 13A, 937-940.
6. Iacoviello, F. and Polini, W. (2000) *La Metallurgia Italiana* 3, 31-34.
7. Iacoviello, F. and Cavallini, M. (2003) *La Metallurgia Italiana* 1, 31-37.